



Published in final edited form as:

Oncogene. 2015 May 21; 34(21): 2801–2806. doi:10.1038/onc.2014.223.

Differential *in vivo* tumorigenicity of diverse *KRAS* mutations in vertebrate pancreas: A comprehensive survey

Joon Tae Park¹, Nicole Johnson¹, Shu Liu¹, Mathieu Levesque¹, Yue J. Wang⁵, Hao Ho³, David Huso⁴, Anirban Maitra³, Michael J. Parsons^{1,2,5}, Jason D. Prescott¹, and Steven D. Leach^{1,2,5}

¹Department of Surgery, Johns Hopkins Medical Institutions, Baltimore, Maryland ²Institute of Genetic Medicine, Johns Hopkins Medical Institutions, Baltimore, Maryland ³Department of Pathology, Johns Hopkins Medical Institutions, Baltimore, Maryland ⁴Department of Molecular & Comparative Pathobiology, Johns Hopkins Medical Institutions, Baltimore, Maryland ⁵Graduate Program in Human Genetics, Johns Hopkins Medical Institutions, Baltimore, Maryland

Abstract

Somatic activation of the *KRAS* proto-oncogene is evident in almost all pancreatic cancers, and appears to represent an initiating event. These mutations occur primarily at codon 12 and less frequently at codons 13 and 61. While some studies have suggested that different *KRAS* mutations may have variable oncogenic properties, to date there has been no comprehensive functional comparison of multiple *KRAS* mutations in an *in vivo* vertebrate tumorigenesis system. We generated a *Gal4/UAS*-based zebrafish model of pancreatic tumorigenesis in which the pancreatic expression of UAS-regulated oncogenes is driven by a *ptf1a:Gal4-VPI6* driver line. This system allowed us to rapidly compare the ability of 12 different *KRAS* mutations (G12A, G12C, G12D, G12F, G12R, G12S, G12V, G13C, G13D, Q61L, Q61R, and A146T) to drive pancreatic tumorigenesis *in vivo*. Among fish injected with one of five *KRAS* mutations reported in other tumor types but not in human pancreatic cancer, 2/79 (0.25%) developed pancreatic tumors, with both tumors arising in fish injected with A146T. In contrast, among fish injected with one of seven *KRAS* mutations known to occur in human pancreatic cancer, 22/106 (20.8%) developed pancreatic cancer. All eight tumorigenic *KRAS* mutations were associated with downstream *MAPK/ERK* pathway activation in preneoplastic pancreatic epithelium, while non-tumorigenic mutations were not. These results suggest that the spectrum of *KRAS* mutations observed in human pancreatic cancer reflects selection based upon variable tumorigenic capacities, including the ability to activate *MAPK/ERK* signaling.

Users may view, print, copy, and download text and data-mine the content in such documents, for the purposes of academic research, subject always to the full Conditions of use:http://www.nature.com/authors/editorial_policies/license.html#terms

Correspondence to: Steven D Leach, MD, Director, David M. Rubenstein Center for Pancreatic Cancer Research, Memorial-Sloan Kettering Cancer Center, 1275 York Ave, Box 20, New York, NY 10065, phone: 646-888-3662, fax: 646-888-3235, leachs@mskcc.org.

Conflict of Interest: The authors declare no conflicts of interest.

Introduction

The *KRAS* proto-oncogene is among the most frequently mutated genes in human tumors. To date, over 300 different *KRAS* mutations have been reported in human cancer (www.sanger.ac.uk/genetics/CGP/cosmic). Among these, base pair substitutions in codons 12, 13, 61 and 146 predominate, with different distributions observed in different tumor types. While these diverse mutations are often felt to have similar biologic significance, it remains to be seen whether they are all able to drive tumorigenesis in an equivalent manner. It is also unclear whether the different distribution of *KRAS* mutations observed in different human cancers reflects tissue-specific differences in mutation occurrence (as might result from differential carcinogen exposure), or to a variable capacity of specific mutations to confer a growth advantage in different tissues.

Among different tumor types, pancreatic cancer is characterized by especially high rates of *KRAS* mutation, with even early, pre-invasive lesions displaying *KRAS* mutation frequencies exceeding 90%¹. To date, only two of these mutations (G12D and G12V) have been functionally evaluated in genetically engineered animal models of pancreatic neoplasia²⁻⁴. While G12D and G12V are the two most common *KRAS* mutations observed in pancreatic cancer, up to 25% of pancreatic tumors will display other mutations, including G12C, G12R, G13D, Q61L and Q61R. Other tumor types, including colon cancer, display additional *KRAS* mutations, including G12A, G12F, G12S, G13C and A146T^{1, 5}. The ability of many of these mutations to drive *in vivo* tumorigenesis has not yet been tested, reflecting the fact that our ability to detect somatic mutations has accelerated at a rate far beyond our ability to experimentally evaluate their functional implications.

As a means to accelerate the functional evaluation of somatic mutations identified in human cancer, the zebrafish has emerged as a promising model organism.^{6, 7} With respect to pancreatic tumorigenesis, stable transgenic zebrafish models of pancreatic cancer have been previously described.⁸ However, the time frame required to generate stable transgenic lines in zebrafish is not fundamentally different from that required in mice, meaning that this approach is not likely to meaningfully alleviate the discrepancy between pancreatic cancer gene discovery and *in vivo* functional evaluation of identified mutations. In order to address this issue, we generated a transient *Gal4-VPI6/UAS* system for functionally evaluating candidate oncogenes in zebrafish pancreas. This has allowed us to effectively compare the ability of 12 different *KRAS* mutations (G12A, G12C, G12D, G12F, G12R, G12S, G12V, G13C, G13D, Q61L, Q61R, and A146T) to drive *in vivo* pancreatic tumorigenesis. In addition to providing insight regarding the varying capacities of different *KRAS* mutations to initiate pancreatic cancer, this system now provides a novel platform for the rapid functional annotation of additional somatic mutations identified in pancreatic cancer genomes.

Results and Discussion

Targeted expression of eGFP-*KRAS*^{mutant} transgenes in zebrafish pancreas

To functionally compare the ability of different human *KRAS* mutations to initiate pancreatic tumorigenesis, twelve different mutations (G12A, G12C, G12D, G12F, G12R,

G12S, G12V, G13C, G13D, Q61L, Q61R, and A146T) were selected for analysis. *KRAS* mutant alleles were generated by modifying a wild-type human *KRAS* cDNA using site-directed mutagenesis followed by full length sequencing to confirm successful mutation. Each mutant variant was expressed as an *eGFP-KRAS^{mutant}* fusion under the transcriptional control of a concatamerized 14×UAS element.⁹ Mosaic pancreatic expression was achieved by injection of *UAS:eGFP-KRAS^{mutant}* constructs into hemizygous *ptf1a:Gal4-VP16* transgenic embryos produced from a cross between the *Tg(ptf1a:Gal4-VP16)^{H16}* BAC transgenic line¹⁰ and wildtype *AB* fish (Fig. 1A). Reflecting known patterns of *ptf1a* gene expression, eGFP expression was first observed in the developing hindbrain and cerebellum (Fig. 1B,C). Due to yolk autofluorescence, pancreas-specific expression of *eGFP-KRAS^{mutant}* transgenes proved to be difficult to detect in whole mount embryos (Fig. 1B and C, asterisk). However, confocal imaging of the micro-dissected pancreas from 5 dpf larvae revealed effective expression and membrane localization of the eGFP-KRAS^{mutant} protein (Fig. 1D-G). On day five, embryos showing eGFP fluorescence within the *ptf1a* expression domain were selected and raised to adulthood.

Relative tumorigenicity of *eGFP-KRAS^{mutant}* transgenes in zebrafish pancreas

At 3 months of age, fish were randomly selected for examination of eGFP fluorescence in the cerebellum and pancreas. All twelve versions of activated *KRAS* were associated with high frequencies of eGFP fluorescence in the cerebellum, as shown for G12D and G12V in Fig. 2A and I. The percentage of fish displaying cerebellar eGFP fluorescence is shown in Fig. 3 (light green bars), and ranged from 44%-100%. As in the case of previously reported *ptf1a:eGFP-KRAS^{G12V}* transgenic fish⁸, no cerebellar or hindbrain tumors were observed in transgenic fish expressing *UAS:eGFP-KRAS^{mutant}* transgenes.

We next sacrificed adult fish with or without transcutaneous eGFP fluorescence in the cerebellum, and examined pancreatic transgene expression as assessed by eGFP fluorescence within dissected abdominal viscera. As in the case of cerebellum, all twelve versions of activated *KRAS* were associated with significant frequencies of pancreatic eGFP fluorescence, ranging from 8%-66.7%. Representative transcutaneous and pancreatic eGFP fluorescence for G12D and G12V are shown in Fig. 2B,C and Fig 2J,K, and additional examples of are shown in Supplemental Fig. S1. Rates of pancreatic eGFP fluorescence are depicted in Fig. 3 (dark green bars), and further immunohistochemical confirmation of *eGFP-KRAS^{mutant}* transgene expression is provided in Figure 4.

Dissected abdominal viscera were then subjected to detailed histological examination in order to determine the presence or absence of pancreatic tumor. The frequencies of pancreatic tumor formation for each version of activated *KRAS* are summarized in Fig. 3 (red bars). Eight out of twelve different *KRAS* mutations were associated with pancreatic tumor formation, typically at frequencies lower than those observed for pancreatic eGFP expression (G12C: 18.2%, G12D: 25%, G12R: 28.6%, G12V: 20%, G13D: 6.7%, Q61L: 20%, Q61R: 7.7%, A146T: 16.7%). In contrast, four out of twelve different *KRAS* mutations (G12A, G12F, G12S and G13C) failed to induce pancreatic tumor formation, even though they were expressed at frequencies equivalent to that observed for fully tumorigenic mutations, as determined by both gross and immunohistochemical examination of eGFP

fluorescence (Figures 3A and 4). No tumors were noted in control *ptf1a:Gal4-VP16* transgenic fish not injected with *eGFP-KRAS^{mutant}* transgenes.

In comparing the ability of different activating *KRAS* mutations to drive tumorigenesis in zebrafish, we noted that all seven mutations previously reported in human pancreatic cancer (G12D, G12V, G12R, G12C, G13D, Q61L and Q61R) were effective in initiating pancreatic tumorigenesis. In contrast, among the five *KRAS* mutations reported in other tumor types but not in human pancreatic cancer (G12A, G12F, G12S, and G13C and A146T) only one (A146T) proved to be tumorigenic in zebrafish pancreas (Figure 3B). Cumulatively, 22/106 fish (20.8%) injected with one of the seven *KRAS* mutations observed in human pancreatic cancer developed pancreatic tumors, compared to 2/79 fish (0.25%) injected with one of the five *KRAS* mutations reported only in other tumor types. These data suggest that the different frequencies observed for different *KRAS* mutations in human pancreatic cancer likely reflect selection based upon variable tissue-specific tumorigenic capacities.

Characterization of pancreatic tumors and assessment of downstream signaling pathways

Representative tumor histologies are presented in Fig. 2 for G12D (Fig. 2D-H) and G12V (Fig. 2L-P), and histologies for all tumors are presented in Supplemental Fig. S1. Among the twenty-two tumors induced by the eight fully tumorigenic versions of oncogenic *KRAS*, there were no major differences in tumor histology. Each tumor displayed predominant features of acinar cell carcinoma, similar to that previously reported for *ptf1a:eGFP-KRAS^{G12V}* transgenic fish⁸, and showed evidence of local tissue invasion and/or metastasis (Supplemental Fig. S2). All tumors also displayed widespread nuclear labeling for PCNA and phospho-ERK (Fig 4A-E and data not shown). In the case of G12V, G12C and G12R, ERK phosphorylation was evident even in residual normal acinar cells adjacent to primary tumors (Supplemental Fig. S3). In contrast, pancreatic tissue from fish injected with non-tumorigenic versions of *KRAS* showed no evidence of histologic abnormality and minimal to no labeling for these markers (Fig. 4F-I). This was true even in spite of widespread oncogene expression, as indicated by eGFP labeling.

Together, these results suggest that, at least in part, the differential frequencies of mutant *KRAS* alleles observed in human pancreatic cancer are reflective of corresponding differences in tumorigenic capacity. This is true in spite of the fact that known oncogenic RAS mutations are all thought to share a common mechanism of stabilizing active RAS:GTP complexes at the expense of inactive RAS:GDP. In the case of mutations in codons 12, 13 or 61, this is achieved through diminished intrinsic GTPase activity¹¹. Other mutations, including those in codons 116 and 119, are associated with a general decrease in RAS protein affinity for guanine nucleotides, shifting the equilibrium towards binding of more abundant GTP¹¹. Despite this unifying biochemical mechanism, RAS family members display highly divergent frequencies of mutation in different tumor types. Activating HRAS mutations promote bladder and salivary gland tumorigenesis, while NRAS mutations are associated with thyroid carcinoma, melanoma and myeloid malignancies¹²⁻¹⁵. Oncogenic *KRAS* mutations, in contrast, are most frequently associated with endodermally-derived tumors, including pancreatic, colorectal and lung carcinomas^{5, 16, 17}. These tissue-specific differences in mutation frequency may reflect both cell lineage-specific differences in

KRAS, *HRAS* and *NRAS* gene expression, as well as unique subcellular localization/compartmentalization patterns associated with each family member¹⁸. In addition, considerable evidence suggests that different mutant *KRAS* alleles may be associated with variable and highly context-dependent downstream effects. In NIH3T3 cells, codon 12 mutations produced stronger protection from apoptosis and enhancement of anchorage-dependent growth compared to codon 13 mutations, even though the two mutations were associated with similar levels of elevated downstream MAP kinase activity¹⁹. Additional studies suggest that specific oncogenic *KRAS* alleles may confer unique chemosensitivity profiles and variable clinical outcomes¹⁹⁻²¹.

Even more compelling evidence suggesting that individual *KRAS* mutant alleles may differ in their tumorigenic capacities is provided by data comparing the prevalence of individual *KRAS* mutations in tumor tissue compared to adjacent normal tissue. In normal human colonic epithelium, the prevalence of codon 12 and codon 13 mutations was found to be nearly equivalent, compared to a 14-fold excess of codon 12 mutations in associated cancers. Similar data are not available regarding the respective rates at which specific *KRAS* mutations arise in human pancreatic tissue. However the current study suggests that, regardless of the rates of their initial appearance, different mutant *KRAS* alleles would be subject to a high degree of selection based on variable tumorigenic capacities.

While the current results clearly suggest *KRAS* allele-specific differences in the ability to induce pancreatic tumor formation, it might be argued that the different rates of tumor formation observed in our study may simply reflect differential expression levels. However we think that this is unlikely to be a primary cause of differential tumorigenicity, as we employed eleven to twenty-five fish in each group to control for fish-to-fish variability in transgene expression, and even non-tumorigenic mutant *KRAS* alleles were associated with high rates of pancreatic eGFP fluorescence. In addition, based on the fact that our assay depends upon mosaic somatic expression, we are likely interrogating large numbers of individual transgene insertion sites, thereby controlling for transgene insertion site-specific influences leading to differential expression. Finally, the fact that those mutations previously identified in human pancreatic cancer were so much more tumorigenic than those not previously observed suggests that the current assay is unlikely to be confounded by arbitrary differences in transgene expression levels. Nevertheless, future initiatives may include comparison of candidate oncogenic mutations (either somatic or germ-line) expressed from an identical genomic locus, as might be achieved through either endonuclease-facilitated homologous recombination^{22, 23} or phiC31-mediated targeted integration²⁴⁻²⁶.

In summary, we have comprehensively surveyed the ability of twelve different oncogenic *KRAS* mutations to induce pancreatic tumors in a novel *in vivo* tumorigenesis assay. Our results suggest that the appearance or non-appearance of individual mutant *KRAS* alleles in human pancreatic cancer is highly associated with the tumorigenic capacity of these mutations in zebrafish. Similar zebrafish-based tumorigenic assays may be useful for *in vivo* functional interrogation of candidate oncogenic mutations identified in other human cancers.

Supplementary Material

Refer to Web version on PubMed Central for supplementary material.

Acknowledgments

The authors wish to thank Mary Chico, Mara Swaim, Anzer Habibullah and Frazer Matthews for expert administrative and technical support. This work was supported by NCI P01 CA134292. SDL was further supported by the Paul K. Neumann Professorship in Pancreatic Cancer at Johns Hopkins University.

References

1. Kanda M, Matthaei H, Wu J, Hong SM, Yu J, Borges M, et al. Presence of somatic mutations in most early-stage pancreatic intraepithelial neoplasia. *Gastroenterology*. 2012; 142:730–733 e739. [PubMed: 22226782]
2. Guerra C, Schuhmacher AJ, Canamero M, Grippo PJ, Verdaguer L, Perez-Gallego L, et al. Chronic pancreatitis is essential for induction of pancreatic ductal adenocarcinoma by K-Ras oncogenes in adult mice. *Cancer cell*. 2007; 11:291–302. [PubMed: 17349585]
3. Hingorani SR, Petricoin EF, Maitra A, Rajapakse V, King C, Jacobetz MA, et al. Preinvasive and invasive ductal pancreatic cancer and its early detection in the mouse. *Cancer cell*. 2003; 4:437–450. [PubMed: 14706336]
4. Aguirre AJ, Bardeesy N, Sinha M, Lopez L, Tuveson DA, Horner J, et al. Activated Kras and Ink4a/Arf deficiency cooperate to produce metastatic pancreatic ductal adenocarcinoma. *Genes & development*. 2003; 17:3112–3126. [PubMed: 14681207]
5. Krasinskas AM, Moser AJ, Saka B, Adsay NV, Chiosea SI. KRAS mutant allele-specific imbalance is associated with worse prognosis in pancreatic cancer and progression to undifferentiated carcinoma of the pancreas. *Modern pathology : an official journal of the United States and Canadian Academy of Pathology, Inc.* 2013; 26:1346–1354.
6. Leach SD. Pisces and cancer: the stars align. *Zebrafish*. 2009; 6:317. [PubMed: 20047464]
7. Yen J, White RM, Stemple DL. Zebrafish models of cancer: progress and future challenges. *Current opinion in genetics & development*. 2014; 24C:38–45. [PubMed: 24657535]
8. Park SW, Davison JM, Rhee J, Hruban RH, Maitra A, Leach SD. Oncogenic KRAS induces progenitor cell expansion and malignant transformation in zebrafish exocrine pancreas. *Gastroenterology*. 2008; 134:2080–2090. [PubMed: 18549880]
9. Davison JM, Akitake CM, Goll MG, Rhee JM, Gosse N, Baier H, et al. Transactivation from Gal4-VP16 transgenic insertions for tissue-specific cell labeling and ablation in zebrafish. *Developmental biology*. 2007; 304:811–824. [PubMed: 17335798]
10. Pisharath H, Parsons MJ. Nitroreductase-mediated cell ablation in transgenic zebrafish embryos. *Methods in molecular biology*. 2009; 546:133–143. [PubMed: 19378102]
11. Barbacid M. ras oncogenes: their role in neoplasia. *Eur J Clin Invest*. 1990; 20:225–235. [PubMed: 2114981]
12. Charbel C, Fontaine RH, Malouf GG, Picard A, Kadlub N, El-Murr N, et al. NRAS Mutation Is the Sole Recurrent Somatic Mutation in Large Congenital Melanocytic Nevi. *The Journal of investigative dermatology*. 2014; 134:1067–1074. [PubMed: 24129063]
13. Fukahori M, Yoshida A, Hayashi H, Yoshihara M, Matsukuma S, Sakuma Y, et al. The associations between RAS mutations and clinical characteristics in follicular thyroid tumors: new insights from a single center and a large patient cohort. *Thyroid : official journal of the American Thyroid Association*. 2012; 22:683–689. [PubMed: 22650231]
14. Parikh C, Subrahmanyam R, Ren R. Oncogenic NRAS rapidly and efficiently induces CMML- and AML-like diseases in mice. *Blood*. 2006; 108:2349–2357. [PubMed: 16763213]
15. Yoo J, Robinson RA. ras gene mutations in salivary gland tumors. *Archives of pathology & laboratory medicine*. 2000; 124:836–839. [PubMed: 10835516]
16. Er TK, Chen CC, Bujanda L, Herreros-Villanueva M. Clinical relevance of KRAS mutations in codon 13: Where are we? *Cancer letters*. 2014; 343:1–5. [PubMed: 24051306]

17. Martin P, Leighl NB, Tsao MS, Shepherd FA. KRAS mutations as prognostic and predictive markers in non-small cell lung cancer. *Journal of thoracic oncology : official publication of the International Association for the Study of Lung Cancer*. 2013; 8:530–542.
18. Prior IA, Hancock JF. Ras trafficking, localization and compartmentalized signalling. *Seminars in cell & developmental biology*. 2012; 23:145–153. [PubMed: 21924373]
19. Guerrero S, Casanova I, Farre L, Mazo A, Capella G, Manges R. K-ras codon 12 mutation induces higher level of resistance to apoptosis and predisposition to anchorage-independent growth than codon 13 mutation or proto-oncogene overexpression. *Cancer Res*. 2000; 60:6750–6756. [PubMed: 11118062]
20. Guerrero SI, Casanova I, FarrÃ© L, Mazo A, CapellÃ© G, Manges R. K-ras Codon 12 Mutation Induces Higher Level of Resistance to Apoptosis and Predisposition to Anchorage-independent Growth Than Codon 13 Mutation or Proto-Oncogene Overexpression. *Cancer Research*. 2000; 60:6750–6756. [PubMed: 11118062]
21. Morelli MP, Kopetz S. Hurdles and Complexities of Codon 13 KRAS Mutations. *Journal of Clinical Oncology*. 2012; 30:3565–3567. [PubMed: 22927534]
22. Auer TO, Duroure K, De Cian A, Concordet JP, Del Bene F. Highly efficient CRISPR/Cas9-mediated knock-in in zebrafish by homology-independent DNA repair. *Genome research*. 2014; 24:142–153. [PubMed: 24179142]
23. Zu Y, Tong X, Wang Z, Liu D, Pan R, Li Z, et al. TALEN-mediated precise genome modification by homologous recombination in zebrafish. *Nature methods*. 2013; 10:329–331. [PubMed: 23435258]
24. Hu G, Goll MG, Fisher S. PhiC31 integrase mediates efficient cassette exchange in the zebrafish germline. *Developmental dynamics : an official publication of the American Association of Anatomists*. 2011; 240:2101–2107. [PubMed: 21805532]
25. Mosimann C, Puller AC, Lawson KL, Tschopp P, Amsterdam A, Zon LI. Site-directed zebrafish transgenesis into single landing sites with the phiC31 integrase system. *Developmental dynamics : an official publication of the American Association of Anatomists*. 2013; 242:949–963. [PubMed: 23723152]
26. Roberts JA, Miguel-Escalada I, Slovik KJ, Walsh KT, Hadzhiev Y, Sanges R, et al. Targeted transgene integration overcomes variability of position effects in zebrafish. *Development*. 2014; 141:715–724. [PubMed: 24449846]

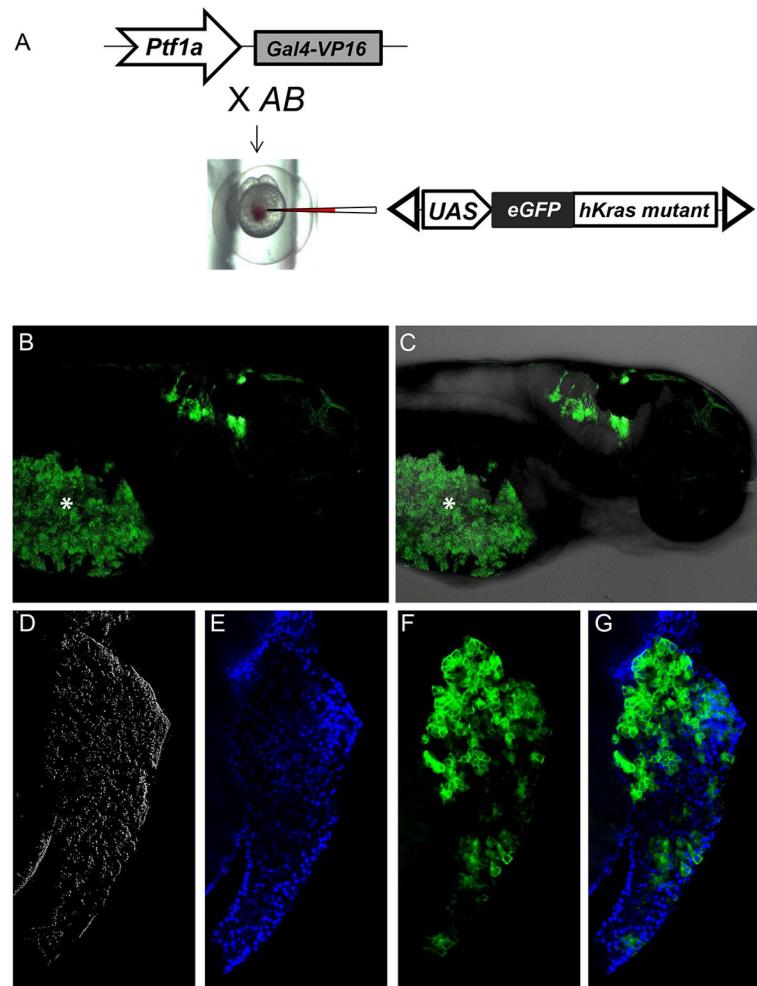


Fig. 1. Targeted expression of *eGFP-KRAS^{mutant}* transgene in zebrafish pancreas
(A) Schematic depiction of experimental design employing the *Gal4-VP16/UAS* system used to drive *eGFP-KRAS^{mutant}* transgene expression within the *ptf1a* expression domain.
(B-C) Lateral view of larval zebrafish (5dpf) under transmitted and fluorescent illumination, showing expression pattern of *eGFP-KRAS^{mutant}* transgene in the hindbrain. Due to yolk autofluorescence (asterisk *), pancreatic expression of the *eGFP-KRAS^{mutant}* transgene is difficult to detect in intact embryos.
(D-G) Confocal image of microdissected pancreas from 5 dpf larval fish, revealing the membrane localization of *eGFP-KRAS^{mutant}* protein. Blue pseudocolor indicates DAPI labeling.

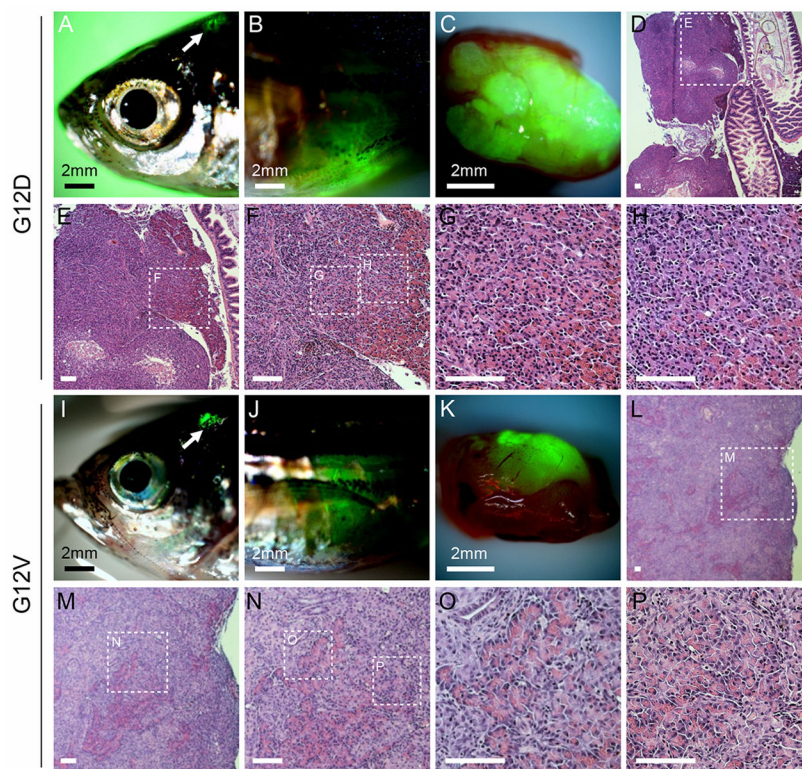


Fig. 2. Identification of Pancreatic Tumors induced by $KRAS^{G12D}$ and $KRAS^{G12V}$
 (A and I) Transcutaneous fluorescence in the cerebellum (white arrow) from $KRAS^{G12D}$ (A), and $KRAS^{G12V}$ (I). (B and J) Transcutaneous fluorescence in the abdomen from $KRAS^{G12D}$ (B), and $KRAS^{G12V}$ (J). (C and K) Dissected abdominal viscera with an eGFP-positive tumor from $KRAS^{G12D}$ (C) and $KRAS^{G12V}$ (K). (D-H, L-P) Histological examination showed the pancreatic acinar tumors from $KRAS^{G12D}$ and $KRAS^{G12V}$. Frank acinar cell carcinoma is interspersed with areas of acinar cell hyperplasia. Boxed areas indicate regions depicted at higher magnification in adjacent images. Scale bars: 50 μ m.

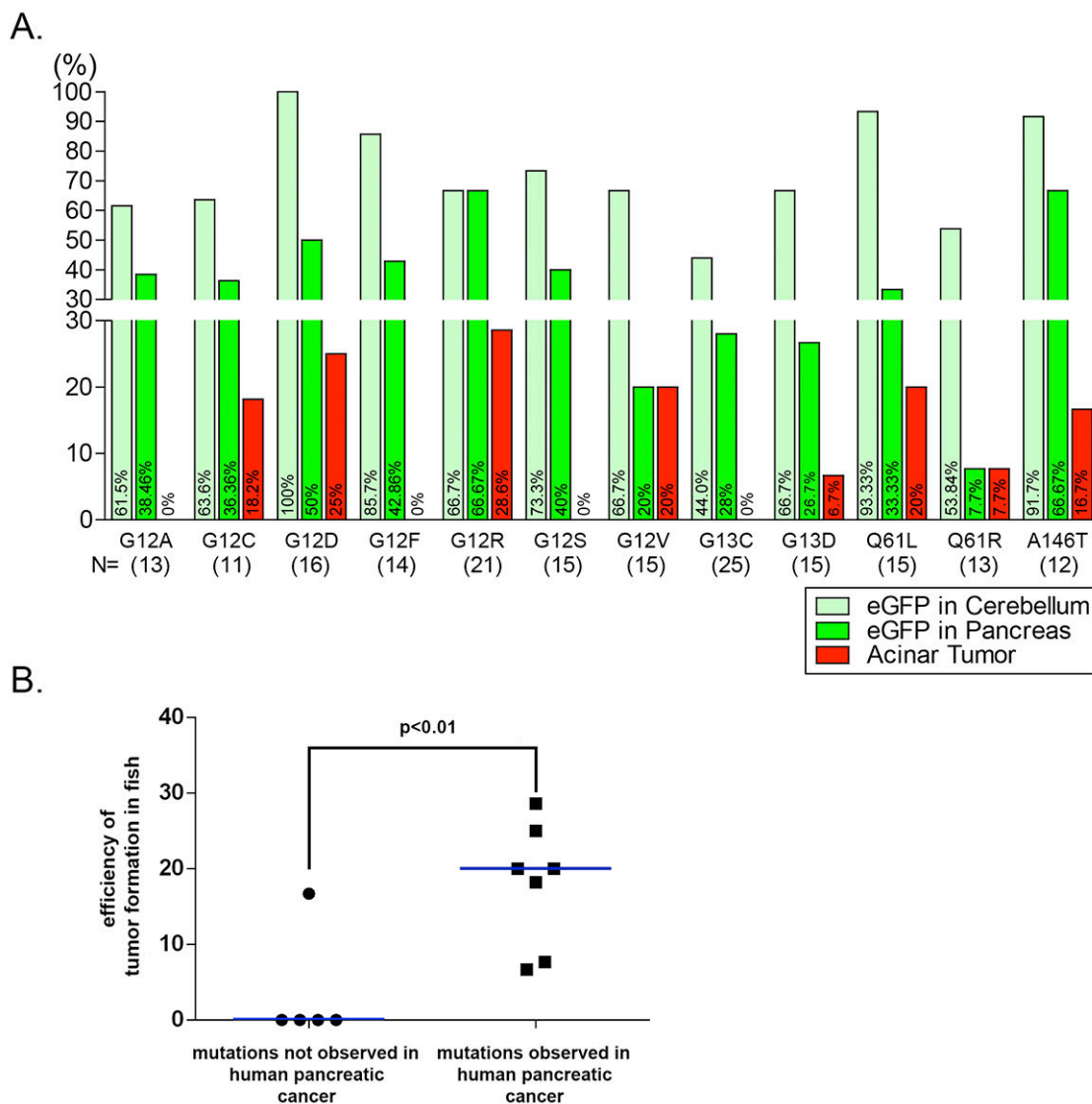


Fig. 3. Comparison of in vivo tumorigenic capacity among twelve different oncogenic *KRAS*^{mutant} alleles

(A) Percentage fish displaying eGFP fluorescence in the cerebellum (light green bars) and pancreas (darker green bars), along with incidence of pancreatic tumor formation at 3 months of age (red bars). Numbers in parentheses indicate number of fish examined for each mutant allele. (B) Comparison of *KRAS* mutant allele-specific efficiency of tumor formation in zebrafish for human *KRAS* mutations previously observed in human pancreatic cancer (n=7) vs. those not previously observed (n=5). Tumor-forming efficiency is significantly greater among mutations previously reported in human pancreatic cancer (p<0.01 by T-test).

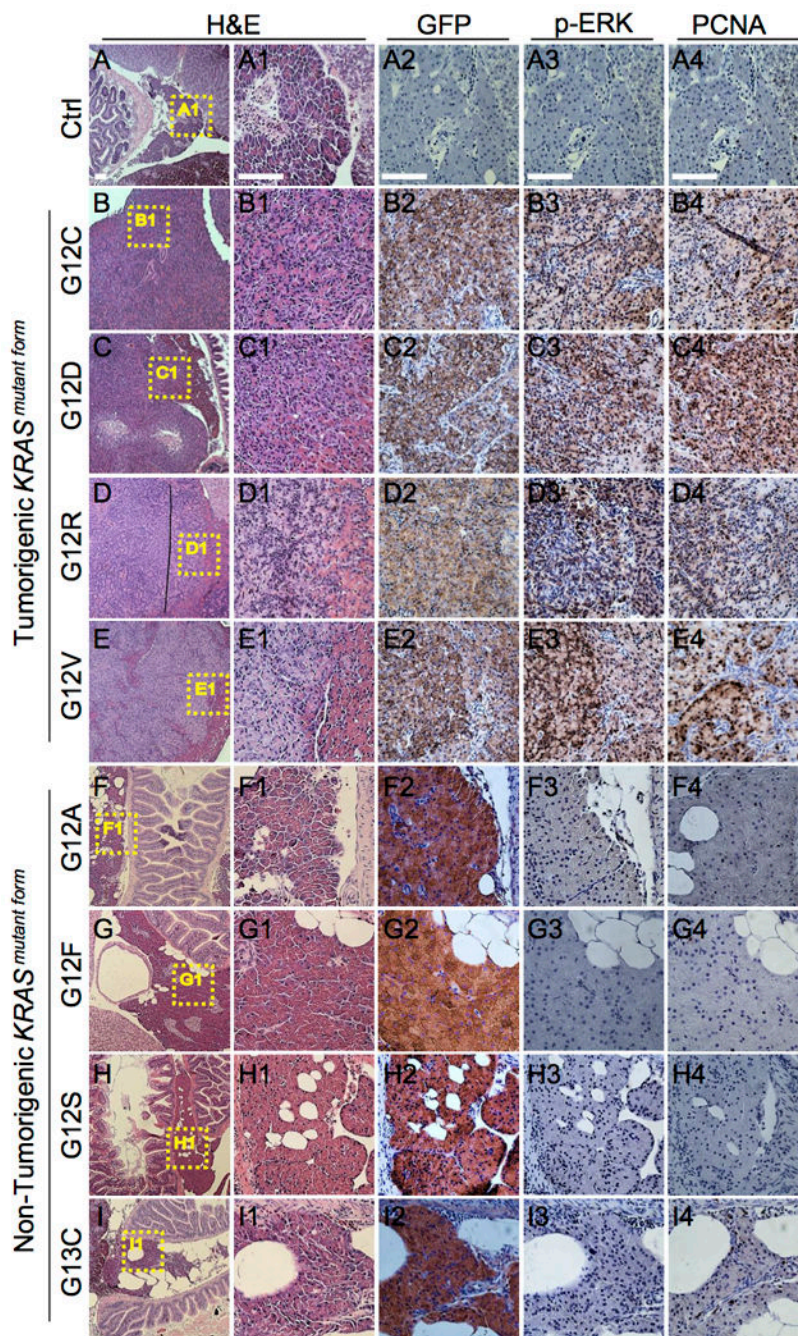


Fig. 4. Characterization of pancreatic tissue expressing tumorigenic and non-tumorigenic $KRAS^{mutant}$ alleles

(A) Pancreatic tissue from uninjected control *ptfla:Gal4-VPI6* fish had histologically normal pancreas and no evidence of tumor formation in any organ. Control pancreatic tissue also displayed no labeling for eGFP and minimal labeling for p-ERK and PCNA. (B-E) Representative pancreatic tissue from fish injected with tumorigenic mutations G12C, G12D, G12R and G12V. Identical results were also observed for fish injected with G13D, Q61L, Q61R, and A146T (data not shown). Resulting tumors were uniformly positive for eGFP and showed strong labeling for p-ERK and PCNA. (F-I) Representative pancreatic

tissue from fish injected with non-tumorigenic mutations G12A, G12F, G12S, and G13C. In spite of widespread expression of *eGFP-KRAS^{mutant}* transgenes, normal histology and minimal labeling for p-ERK and PCNA are observed. Regions outlined by dotted lines indicated areas depicted at higher magnification in adjacent images. Primary antibodies used for immunohistochemistry were rabbit anti-eGFP (Invitrogen, A11122, 1:400), rabbit anti-phospho-ERK (Cell Signaling Technology, 4370S, 1:400), and mouse anti-PCNA (DAKO, M0879, 1:400).

Author Manuscript

Author Manuscript

Author Manuscript

Author Manuscript